Deficiency in kinesin-1 recruitment to melanosomes precludes it from facilitating their centrifugal transport

Christopher L. Robinson[1], Richard D. Evans[1], Deborah A. Briggs[1], Jose S, Ramalho[2] and Alistair N. Hume[1]*

[1]School of Life Sciences, University of Nottingham, Nottingham, NG7 2UH, UK. [2]CEDOC Faculdade de Ciencias Medicas, Universidade Nova de Lisboa, 1169-056 Lisbon, Portugal

* address correspondence to Alistair.hume@nottingham.ac.uk

Key words: organelle transport; kinesin-1, myosin-Va; actin; microtubules; melanocyte

Summary Statement.

We show that Kif5b can compensate for defects in myosin-Va-based transport in mammals, but that endogenous Kif5b plays little role in transport in melanocytes due to inefficient recruitment to melanosomes.

Journal of Cell Science • Advance article

JCS Advance Online Article. Posted on 10 May 2017

Abstract.

Microtubules and F-actin, and associated motor proteins, are considered to play complementary roles in long- and short-range organelle transport. However, there is growing appreciation that myosin/F-actin networks can drive long-range transport. In melanocytes myosin-Va and kinesin-1 have both been proposed as long-range centrifugal melanosome transporters. Here we investigated the role of kinesin-1 heavy chain (Kif5b) and its suggested targeting factor Rab1a in transport. Using confocal microscopy and sub-cellular fractionation we did not detect Kif5b or Rab1a on melanosomes. Meanwhile functional studies, using siRNA knockdown and dominant negative mutants, did not support a role for Kif5b or Rab1a in melanosome transport. To probe the potential of Kif5b to function in transport we generated fusion proteins that target active Kif5b to melanosomes and tested their ability to rescue perinuclear clustering in myosin-Va deficient cells. Expression of these chimeras, but not full length Kif5b, dispersed melanosomes with similar efficiency to myosin-Va. Our data indicate that kinesin/MT can compensate for defects in myosin-Va/actin-based transport in mammals but that endogenous Kif5b plays little role in transport in melanocytes due to its inefficient recruitment to melanosomes.

Introduction.

Actin and microtubule cytoskeleton tracks and their associated motor proteins regulate intracellular organelles transport in eukaryotes (Alberts et al., 2008, Barlan et al., 2013, Ross et al., 2008). Microtubules emanate from the centrosome, or microtubule organising centre, with their fast-growing 'plus' ends oriented towards the plasma membrane and their slow growing 'minus' ends focused at the centrosome. Thus minus end directed dynein and plus-end directed kinesin motors may transport cargo over long distances (>1μm) along these tracks (Hirokawa et al., 2009, Kardon and Vale, 2009). In contrast the actin cytoskeleton in animal cells typically appears to be comprised of a complex network of short (<1μm) randomly oriented filaments suggesting that myosin motors tether or move cargo only short distances (Woolner and Bement, 2009, Wu et al., 1998). These observations are the cornerstone of the 'highways and local roads' model for transport along MTs and actin tracks (Woolner and Bement, 2009). Previously, this model has been supported by studies of the transport of various intracellular cargoes including melanosomes in mouse melanocytes (Ross et al., 2008, Goode et al., 2000, Hume et al., 2011, Fukuda, 2013, Hammer and Sellers, 2012). Elegant studies that used the FK506 binding protein (FKBP)-rapamycin-FKBP/rapamycin binding protein (FRB) to specifically recruit myosin and kinesin/dynein motors to peroxisomes in COS-7 cells came to similar conclusions i.e. microtubule motors drive long-range organelle transport from the cell centre to the periphery, while myosin motors move cargo locally at the cell periphery (Barlan et al., 2013, Goode et al., 2000, Kapitein et al., 2013, Ross et al., 2008). Nevertheless, there is also evidence from several systems that actin/myosin networks can drive organelle transport and positioning over long distances in the absence of microtubules. For instance, in yeast Myo2 transports cargo including vacuoles and secretory vesicles along actin bundles into the bud (Pruyne et al., 2004), while in murine oocytes endosomes organise a network of actin filaments that allow their myosin-Vb dependent transport to the plasma membrane (Schuh, 2011, Holubcova et al., 2013).

Skin melanocytes reside in the hair follicles and the basal layer of the epidermis. There they synthesise pigment in lysosome-related organelles, termed melanosomes, which they then distribute to neighbouring keratinocytes via a network of dendrites (Fukuda, 2013, Hume et al., 2011, Raposo and Marks, 2007). Early studies revealed that the dendrites of melanocytes derived from the myosin-Va null (dilute) mouse were devoid of pigment, suggesting a role for myosin-Va in transporting melanosomes into dendrites or tethering them there (Provance et al., 1996, Wei et al., 1997). Later studies revealed that a sub-population of melanosomes in dilute melanocytes undertake bi-directional transport along microtubules that extend along the length of the dendrites. However, this transport was insufficient to allow peripheral accumulation of melanosomes suggesting that myosin-Va tethers (or 'captures') melanosomes at the dendrite tip by attaching them to randomly oriented actin filaments and prevents them from returning to the cell body (Wu et al., 1998). This 'co-operative capture' model for melanosome transport proposed that melanosomes accumulate in dendrites by sequential long-range transport along microtubules, and myosin-Va/actin dependent tethering at the periphery. Follow-up studies revealed that the small GTPase Rab27a and its effector melanophilin recruit and activate myosin-Va at the melanosomes (Wu et al., 2002, Hume et al., 2001, Fukuda et al., 2002). In line with the co-operative capture model contemporaneous studies also suggested that kinesin-1 and cytoplasmic dynein associate with melanosomes and drive their microtubule-dependent movement and transfer to keratinocytes (Vancoillie et al., 2000a, Vancoillie et al., 2000b, Byers et al., 2000, Hara et al., 2000). More recent studies have revisited to this topic and have proposed that melanosomal recruitment of dynein/dynactin is regulated by Rab36, melanoregulin and Rab7 effector RILP (Rab interacting lysosomal protein) (Matsui et al., 2012, Ohbayashi et al., 2012).

We previously tested the co-operative capture model by directly examining the role of microtubules and F-actin/myosin-Va in melanosome transport (Evans et al., 2014). We found that, although video-microscopy reveals that ~10% of melanosomes in wild-type melanocytes move bi-directionally on microtubules at steady-state, microtubule integrity was only essential for centripetal, and not

centrifugal, transport (Evans et al., 2014, Hume et al., 2011). Instead we found that centrifugal transport was driven by myosin-Va working in concert with a pool of dynamic F-actin and that this process was accelerated in cells depleted of microtubules, suggesting that microtubule and F-actin transport mechanisms oppose one another. Moreover isoform-specific adaptations, e.g. lever arm length and dynamic interaction with F-actin, which allow myosin-Va to move processively towards the +/barbed ends of F-actin in vitro, were essential for its function in melanocytes. These observations indicate that myosin-Va is a transporter that works with a dynamic F-actin network, polarised towards the cell membrane, to move melanosomes to the cell periphery, and not a tether as previously suggested (Wu et al., 1998). As microtubules are tracks for kinesin and dynein motors, our data also support an essential role for cytoplasmic dynein in centripetal transport but not kinesin-1, or other +end directed motors, in centrifugal transport.

In contrast two recent reports proposed that the small GTPase Rab1a (previously shown to have a highly conserved function in ER-Golgi transport (Tisdale et al., 1992, Segev et al., 1988) can recruit kinesin-1 heavy chain Kif5b (hereafter Kif5b) to melanosomes, via its effector SKIP/PLEKHM2 (SifA and kinesin interacting protein/Pleckstrin homology domain-containing family M 2) and KLC2 (kinesin light chain 2), and thereby regulate microtubule-dependent centrifugal melanosome transport (Ishida et al., 2015, Ishida et al., 2012). Consistent with this hypothesis these studies showed that siRNA knockdown of these proteins individually resulted in perinuclear melanosome clustering albeit in only 20-40% of transfected cells. Meanwhile co-expression of constitutively active Rab1a mutant ($Rab1a^{Q70L}$) and SKIP resulted in peripheral accumulation of melanosomes in 25% of cells. Overall these observations provide some support to the idea that Kif5b might be a driver of centrifugal melanosome transport.

To try to resolve this controversy here we tested head-on the role of Kif5b and Rab1a in melanosome transport by investigating their localisation and function in melanocytes. Our results indicate that neither protein is enriched at the melanosome membrane and that neither plays a

detectable role in melanosome transport. On the contrary we found that fusion proteins that forcibly direct active Kif5b to melanosomes can efficiently disperse clustered melanosomes along microtubules in myosin-Va deficient melanocytes. We suggest that myosin-Va, and not Kif5b, is the dominant centrifugal transport in melanocytes and that the limited capacity of melanosomes to recruit Kif5b restricts its function in this process.

Results.

The distribution of Kif5b and Rab1a within melanocytes is inconsistent with their proposed role in melanosome transport.

As a first step to investigate the possible role of Kif5b and Rab1a in centrifugal melanosome transport we investigated their intracellular localisation in melanocytes. To do this we transiently expressed GFP-Rab1a and Kif5b-YFP fusion proteins in immortal wild-type mouse melanocytes (melan-a) and then used confocal immunofluorescence microscopy (CIFM) to examine their localisation relative to melanosomes. Previous studies found that a GFP-Rab1a could rescue Golgi fragmentation in HeLa cells depleted of endogenous Rab1a (Aizawa and Fukuda, 2015). Meanwhile Kif5b-YFP maintained localisation with MT1-MMP, whose surface expression is regulated by Kif5b, in MDA-MB-231 cells (Marchesin et al., 2015). These observations indicate that these fusion proteins retain function. In contrast to GFP-Rab27a, neither Kif5b-YFP nor GFP-Rab1a was enriched in areas containing melanosomes, detected using phase contrast and anti-tyrosinase staining (Figure 1A, B and D). Instead much of the Kif5b-YFP, like GFP alone, appeared to be distributed uniformly throughout the cytoplasm with a sub-set accumulated in peripheral spots that are likely to correspond to the fast growing plus-tips of microtubules which are located in dendrite tips (Figure 1B and C) (Hume et al., 2007, Wu et al., 2005). This is consistent with the ability of Kif5b motor protein to move processively towards the plus-ends of microtubules (Hirokawa et al., 2009). In line with these observations co-localisation analysis revealed no significant difference in the overlap between tyrosinase and Kif5b-YFP or GFP alone (mean PCC = 0.457 +/- 0.07125 for Kif5b-YFP, versus

0.3691 +/- 0.1183 for GFP). In contrast, and consistent with its role in melanosome transport, Rab27a exhibited significantly higher level of colocalisation with tyrosinase (mean PCC = 0.701 +/- 0.084; Figure 1F).

In parallel we used immunoblotting to test the relative abundance of endogenous Kif5b in a melanosome enriched (P17,000) fraction of melan-a cells, using Kif5b specific antibodies. Blotting using anti-tyrosinase antibodies, and comparison of the intensity of band for P17,000 and S17,000 fractions confirmed melanosome enrichment in P17,000 relative to S17,000. Meanwhile comparison of the intensities of Kif5b-specific bands in P17,000 and S17,000 revealed the opposite i.e. that Kif5b was enriched in a fraction containing low density organelles and cytosol (S17,000) and not in tyrosinase/melanosome enriched P17,000 fraction. The reciprocal intensities of the bands for Kif5b and tyrosinase in these fractions indicates that at most only a small fraction of Kif5b associates with melanosomes at steady state (Figure 1G).

CIFM revealed that GFP-Rab1a was mostly distributed in the perinuclear cytoplasm consistent with its highly conserved role in regulating endoplasmic reticulum to Golgi transport (Figure 1D-E) (Tisdale et al., 1992, Nuoffer et al., 1994). In support of this we found that the intracellular distribution of GFP-Rab1a correlated significantly more closely with that of endogenous giantin, a Golgi matrix protein, than tyrosinase (Mean PCC = 0.795 +/- 0.084 for giantin, versus 0.443 +/- 0.087 for tyrosinase; Figure 1E and H) (Linstedt and Hauri, 1993).

Thus our data indicate that Rab1a and Kif5b are unlikely to strongly associate with melanosomes in melanocytes. Given that proteins e.g. Rab27a and myosin-Va, which have well-established roles in regulating melanosome transport co-localise with these organelles (Figure 1F) (Hammer and Sellers, 2012, Hume and Seabra, 2011), the lack of apparent association between melanosomes, Rab1a and Kif5b argues against a direct role for these proteins in melanosome transport. In line with this we found that a motor-less version of Kif5b (GFP-Kif5bΔ350) distributed in a filament-like pattern throughout the cytoplasm (that may correlate with microtubules), while myc-tagged SKIP

accumulated in the peripheral cytoplasm, consistent with its previously reported Kif5b dependent dispersion (Rosa-Ferreira and Munro, 2011, Navone et al., 1992). Thus neither displayed obvious co-localisation with melanosomes in (Figure S1A).

Functional disruption of Kif5b affects centrifugal transport of mitochondria, but not melanosome in melanocytes.

To test the function of Kif5b in transport we used siRNA to deplete Kif5b in melanocytes and then examined the effects of this on two read-outs of centrifugal transport; 1) maintenance of dispersed melanosome distribution in melan-a cells, and 2) myosin-Va-dependent dispersion of perinuclear melanosome clustering in myosin-Va-null (melan-d1) cells. Western blotting confirmed that several pairs of siRNA oligonucleotides were effective in depleting Kif5b protein (Figure 2A). [These siRNA included sequences used previously to deplete these targets; (Ishida et al., 2015, Ishida et al., 2012, Gupta et al., 2008a) (See methods for details.)].

In the first centrifugal transport assay (maintenance of dispersed melanosome distribution in melan-a cells) control siRNA depletion of Rab27a resulted in perinuclear melanosome clustering in a significant majority of melan-a cells (Figure 2B-C; cells with clustered melanosomes = 85.26+/-9.038% for Rab27a, versus 13.88+/-15.60% for non-targeted (NT) control siRNA transfected cells), while Kif5b specific siRNA did not. This indicates that unlike Rab27a and its effectors (melanophilin and myosin-Va), Kif5b does not play a significant role in centrifugal transport.

Similarly in the second centrifugal transport assay (myosin-Va-dependent dispersion of perinuclear melanosome clustering in myosin-Va-null (melan-d1) cells) siRNA depletion of Rab27a significantly reduced myosin-Va-dependent dispersion of perinuclear clustered melanosomes compared with control siRNA transfected cells, while Kif5b specific siRNA did not (Figure 3A-B; rescued cells = 13.45 +/- 6.426% for Rab27a, versus 89.41 +/- 5.428% for NT transfected cells).

This further indicates that expression of Rab27a (and its effectors melanophilin and myosin-Va), but not Kif5b, is required for centrifugal melanosome transport in melanocytes (Fukuda, 2013, Hume et al., 2011). To confirm that the level of Kif5b knockdown was sufficient to block its function we examined the distribution of mitochondria and GFP-SKIP in siRNA transfected melanocytes. Previous studies revealed perinuclear accumulation of mitochondria in knockout cells and reduction in accumulation of GFP-SKIP at the cell periphery in Kif5b depleted HeLa cells, indicating that Kif5b functions in centrifugal transport of mitochondria and GFP-SKIP (Dumont et al., 2010, Tanaka et al., 1998). Consistent with this, we observed perinuclear clustering of mitotracker labelled mitochondria and reduction in peripheral localised GFP-SKIP in wild-type melanocytes transfected with Kif5b, but not Rab27a or control (NT), siRNA (Figure 2B, S1C).

Functional disruption of Rab1a affects the integrity of the Golgi apparatus but not centrifugal melanosome transport in melanocytes.

To probe the role of Rab1a in melanocytes we tested the effect of over-expression of mutants that alter its GDP/GTP exchange and GTPase activity; Rab1a^{N124I} (nucleotide-free form) and Rab1a^{Q70L} (constitutively GTP-bound form). We found that expression of the inactive Rab1a^{N124I} mutants, but not wild-type or constitutively active (CA) Rab1a^{Q70L}, resulted in fragmentation of the Golgi apparatus in a significant proportion of cells (44.22 +/- 9.584% for Rab1aN124I versus 2.564 +/- 4.441% for GFP). This is consistent with the reported ability of this mutant to disrupt Rab1a function in ER to Golgi trafficking (Wilson et al., 1994). Conversely, we found that expression of CA Rab1a^{Q70L}, but not wild-type Rab1a or inactive Rab1a^{N124I}, triggered melanosome clustering in a significant proportion of cells, albeit with significantly lower efficiency than the Rab27a-binding domain of melanophilin (Mlph-RBD = 90.88 +/- 13.26% versus Rab1a^{Q70L} = 65.05 +/- 11.8%; Figure 4).

Overall these data do not support a positive role for Kif5b or Rab1a in driving melanosome dispersion. Indeed the ability of the Rab1a^{Q70L} mutant to cause melanosome clustering, shown here and previously, support the possibility that Rab1a functions in a process that opposes centrifugal transport (Ishida et al., 2015, Ishida et al., 2012).

Forced targeting of Kif5b to melanosomes drives their microtubule-dependent dispersion.

As an alternative approach to investigate the function of Kif5b in transport we tested the effect of GFP-Kif5b expression in myosin-Va deficient melan-d1 cells. We found that GFP-Kif5b did not co-localise with, or disperse melanosomes to a significantly greater extent than GFP alone (mean pigment area = 25.32+/- 6.356% for GFP-Kif5b, versus = 32.02 +/- 5.325% for GFP; Figure 5A+B). This further suggests that Kif5b does not transport melanosomes.

One possible explanation for the lack of effect of Kif5b on transport is that there is an essential requirement for actin/myosin-Va in centrifugal transport that cannot be overcome by kinesin/microtubules-dependent transport. Alternatively, melanosomes may have limited capacity to recruit Kif5b. To investigate these possibilities we generated fusion proteins between Kif5b, myosin-Va and other melanosome targeting proteins and tested their function and localisation in melan-d1 cells. A similar approach, re-tasking fission yeast kinesin-7 (Tea2) to transport type V myosin (Myo52) cargo along microtubules, has been used to show that transport on microtubules can restore polarised growth and viability in cells lacking actin cables, that are the physiological tracks for Myo52 cargo (Lo Presti and Martin, 2011).

To target active Kif5b (an N-terminus 1-810 amino acid fragment containing the motor, neck/linker and stalk regions but lacking the C-terminus cargo binding/regulatory tail) to melanosomes we used two strategies (Figure 5A). Firstly, we modified the previously described “mini-myosin” (mini-Va) vector such that the myosin-Va S1 (motor/lever arm) encoding fragment was replaced by active

Kif5b. This protein termed “mini-K5b” targets to melanosomes via the RBD of Rab27a effector synaptotagmin-like protein 2-a (Sytl2a) (Figure 5A-C). Secondly, we generated a K5b-MVa fusion protein, comprising (from the N-terminus); GFP, active Kif5b, and the melanosome binding tail fragment of myosin-Va (Strom 2002; Figure 5A). K5b-MVa, like myosin-Va, targets to melanosomes via the interaction of the myosin-Va tail with endogenous melanophilin. [Consistent with this K5b-MVa and full length myosin-Va, in contrast to mini-Va and mini-K5b, were non-functional in melanophilin deficient melan-ln cells (Figure S2).] In parallel we engineered the reciprocal MVa-K5b fusion protein comprising (from the N-terminus); 1) GFP, 2) the myosin-Va S1, and 3) motor-less Kif5b (i.e. a fragment that contains the neck/linker, stalk and cargo/light chain binding tail) (Figure 5A).

In line with previous studies we found that full-length myosin-Va and mini-Va localised to/and dispersed significantly melanosomes in melan-d1 cells compared with GFP alone (mean pigment area; myosin-Va = 87.21 +/- 6.94% and mini-Va = 76.59 +/- 11.97%; Figure 5D; Evans et al 2014). In contrast MVa-K5b did not rescue melanosome distribution or localise to melanosomes, and instead localised to actin-rich cell periphery where it accumulated at the distal tips of filopodia-like extension, confirming the activity of the myosin-Va fragment (Figure 5B-C). This is consistent with the lack of co-localisation between melanosomes and GFP-Kif5b and motor-less Kif5b (GFP-Kif5bΔ350) (Figures S1A and 5B-C), and suggests that Kif5b function in melanosome transport is restricted by the limited capacity of melanosomes to recruit this motor.

In accord with this we observed that mini-K5b and K5b-mVa both localised to, and dispersed melanosomes with similar efficiency to myosin-Va and mini-Va (mean pigment area; mini-K5b = 80.18 +/- 14.26 and K5b-MVa = 86.37 +/- 11.33). However, in contrast to myosin-Va and mini-Va, and in line with the role of Kif5b as a microtubule motor, their activity was dependent upon microtubule integrity (mean pigment area in microtubule depleted cells; mini-K5b = 46.84 +/- 12.05%, K5b-MVa = 47.82 +/- 3.271%, GFP = 36.45 +/- 9.469% versus myosin-Va = 78.42 +/- 9.144%

and mini-Va = 57.5 +/- 16.55%; Figure S3). Further supporting the microtubule dependence of mini-K5b and K5b-MVa driven transport we observed that in many cells expressing these proteins melanosomes accumulated in the tips of dendrites and were relatively depleted in the central cell cytoplasm (see Figure S4A for an example). This is consistent with the role of Kif5b as a +end directed motor and the peripheral distribution of microtubule +ends in melanocytes.

Collectively these data indicate that Kif5b can disperse melanosomes with similar efficiency to myosin-Va, but that its capacity to do so is restricted by the limited ability of its cargo binding tail to associate with melanosomes.

Discussion.

Here we probed the role of Kif5b and Rab1a in centrifugal melanosome transport in melanocytes. Our main findings are two-fold.

Firstly, we were unable to find evidence that Kif5b or Rab1a contribute to centrifugal melanosome transport. Using several pairs of siRNA oligonucleotides we found that knockdown of Kif5b (the most abundant kinesin-1 heavy chain in melanocytes) did not affect the dispersed distribution of melanosomes in wild-type melanocytes or the ability of GFP-myosin-Va to rescue melanosome clustering in myosin-Va deficient melan-d1 cells, both read-outs of centrifugal transport (Figure 2-3). Meanwhile disruption of Rab1a function by expression of the dominant negative mutant Rab1a^{N124I} did not affect melanosome distribution in wild-type melanocytes, arguing against its role in promoting their centrifugal transport (Figure 4). The latter possibility is further undermined by the observation that expression of the constitutively active Rab1a^{Q70L} caused melanosome clustering in wild-type cells (Figure 4; Ishida 2012). Together with the lack of obvious association between Kif5b/Rab1a and melanosomes (Figure 1), these data suggest that Kif5b and Rab1a contribute less significantly than myosin-Va to centrifugal transport. This chimes with our previously published data showing 1) that microtubule integrity is not essential for centrifugal transport driven by myosin-Va and dynamic actin, and 2) that only 10% of melanosome movements in wild-type melanocytes were microtubule dependent (Evans et al., 2014, Hume et al., 2011). Similar results have been reported regarding the contribution of microtubules to centrifugal transport in amphibian melanophores, indicating that myosin-Va/F-actin likely play an important role in melanosome transport in multiple species. (Gross et al., 2002, Rogers and Gelfand, 1998, Schliwa and Euteneuer, 1978). Furthermore in preliminary experiments we found that transfection of wild-type melanocytes with siRNA pools targeted against each of the 46 mouse kinesin heavy chains genes had no detectable effect on melanosome dispersion (A Hume, I Meschede and M. Seabra unpublished observations).

Together the data presented here and previously suggests that microtubules and +end directed kinesins, e.g. Kif5b, are not the main drivers of centrifugal transport.

Secondly, we found that the role of Kif5b in transport is limited by the capacity of melanosomes to recruit the motor. We saw that although an active Kif5b motor/stalk fragment could disperse melanosomes in melan-d1 cells when artificially targeted there by replacement of the endogenous tail with the Rab27a binding domain of sytl2-a (mini-K5b), or the melanophilin binding tail of myosin-Va (K5b-MVa), this was not the case for proteins containing the endogenous Kif5b tail (Figure 1, 5, S1A). The latter finding is consistent with the negative results of our functional studies of Kif5b and Rab1a in melanosome transport, and suggests that dearth of targeting factors limits Kif5b function in this process (Figure 2-4).

Interestingly, in many cases expression of artificially melanosome targeted kif5b protein resulted in hyper-accumulation of melanosomes in the peripheral cytoplasm (Figure S4A). A similar phenomenon, termed 'peripheral melanosome aggregation', was observed in other studies in a subset (~25%) of melan-a cells in which Rab1a^{Q70L} and SKIP were co-expressed (Ishida et al., 2015). In contrast, as shown here and previously, individual expression of Rab1a^{Q70L} and SKIP causes 1) melanosome clustering, and 2) dispersion of lysosomes, respectively (Ishida et al., 2015, Ishida et al., 2012, Rosa-Ferreira and Munro, 2011, Dumont et al., 2010) (Figure 4 and S1B). In lysosome dispersion SKIP acts as an adaptor allowing Arl8b to recruit Kif5b to lysosomes. Recent data, showing SKIP interacts with Rab1a^{Q70L}, suggests that a similar mechanism underlies SKIP driven dispersion of the Golgi apparatus i.e. SKIP acting as an adaptor allowing active Rab1a to recruit Kif5b to the Golgi apparatus. Although the mechanism of Rab1a^{Q70L} mediated melanosome clustering is unclear, it was previously shown (and confirmed here) that Rab1a^{Q70L} can associate with melanosomes and thus could disperse melanosomes by recruiting SKIP and Kif5b ((Ishida et al., 2015, Ishida et al., 2012) (Figure S4B). However, the observation that dual SKIP/Rab1a^{Q70L} expression is required for dispersion suggests that physiological levels of SKIP in melanocytes are insufficient to allow melanosomal,

active Rab1a to recruit enough Kif5b to disperse melanosomes. Conversely, the finding that SKIP expressed alone does not localise to, or affect the distribution of melanosomes, suggesting that melanosomes contain low levels of active Rab1a compared the Golgi apparatus. This further supports the idea that the Rab1a/SKIP/KLC2/Kif5b axis does not play a significant role in transport in the absence of over-expression.

Finally, how do we reconcile our conclusion that Kif5b is not a significant melanosome transporter with previous studies which proposed that Kif5b, recruited by Rab1a, SKIP and KLC2, regulates microtubule-dependent centrifugal melanosome transport (Ishida et al., 2015, Ishida et al., 2012)? One possibility is that the level of knockdown achieved in our study, although sufficient to affect transport of mitochondria and GFP-SKIP, was insufficient to affect Kif5b function in melanosome transport. This might be the case if relatively few motors were required to move melanosomes compared with other cargo. Another possibility is that the cells used here and previously (Ishida et al., 2015, Ishida et al., 2012) differ in their ability to recruit Kif5b to melanosomes. While we cannot exclude this possibility it is noteworthy that neither of the previous studies directly tested the ability of Kif5b to associate with melanosomes nor did they directly test the requirement for Kif5b in melanosome dispersion. Leading from this, while we agree that melanosome clustering seen in the previous studies in Kif5b etc, depleted cells is consistent with a role for these proteins in microtubule-dependent centrifugal transport, we consider that caveats remain regarding this conclusion. Firstly, it is not clear that the observed clustering is due to defects in microtubule dependent transport rather than an indirect effect of disrupting the F-actin/myosin-Va transport system. We suggest that to conclude the former it would be essential to test whether the rescue of clustering, i.e. centrifugal melanosome transport, is microtubule dependent. Secondly, if Kif5b is an essential regulator of centrifugal melanosomes transport, it is not clear why clustering was observed in only 20-40% of depleted cells. In contrast depletion of Rab27a, results in clustering in 80-100% of transfected cells (Figures 2-3). Indeed the low proportion of clustering observed in Kif5b depleted cells is particularly surprising given that the depletion of the siRNA target proteins seen in Western

blotting appears greater than 20-40% (Ishida et al., 2015). Thirdly, we were unable to reproduce the melanosome clustering observed in those studies using the same cell line and the same oligonucleotides. In conclusion, while we cannot totally exclude a role for Kif5b in melanosome transport, our data presented here and previously do not support an essential role for it in this process.

Methods.

Cell culture and transfection. Cultures of immortal melan-a, melan-d1 and melan-ln melanocytes were maintained and transfection with plasmid and siRNA oligonucleotides as described previously (Evans et al 2014; Hume et al 2007). For depletion of microtubules cells were cultured in growth medium supplemented with nocodazole 10μM.

Plasmid and virus constructs. Generation of plasmid vectors pEGFPC3-Rab27a and pEGFPC3-Rab1a and adenovirus allowing expression of GFP-Rab27a, GFP-Rab1a and GFP-myosin-Va (melanocyte isoform) in melanocytes were previously described (Evans et al., 2014, Hume et al., 2001). pENTR-GFPC2-KIf5bΔ350 and pENTR-GFPC2-SKIP allowing expression of GFP-KIf5bΔ350 and GFP-SKIP were generated in the course of this study. pEYFPN1-KIF5B allowing expression of human Kif5b at the N-terminus of YFP, generated by Dr Chen Gu (Ohio State University, USA) as described previously (Gu et al., 2006), was gifted to us by Dr Stefan Linder (Hamburg, Germany). pENTR-myc-SKIP allowing expression of SKIP tagged at the N-terminus with the myc epitope was gifted to us by Dr Sean Munro (MRC-LMB Cambridge). To investigate the role of Kif5b and Rab1a in melanosome transport and its targeting to melanosomes adenovirus vectors were generated that allow expression of the following fusion proteins in melanocytes; GFP-Kif5b, mini-K5b, K5b-MVa, MVa-K5b, GFP-Rab1a, GFP-Rab1a^{Q70L} and GFP-Rab1a^{N124I} as described previously (Hume et al., 2006). Adenoviruses allowing expression of melanophilin-RBD, mini-Va and full-length myosin-Va, containing the melanocytes specific exons D and F, were previously described (Evans et al., 2014, Hume et al., 2006). Primer sequences and further details of the cloning procedures used are available on request.

Immunoblotting. Immunoblotting was performed as described previously (Hume et al., 2007) using goat anti-Kif5b (Everest Biotech EB05492; 1:1000), goat anti-GAPDH (Sicgen Ab0049-200; 1:5000) and rabbit anti-tyrosinase (PEP7 a kind gift from Dr Vincent Hearing, NCI-NIH, USA; 1:1000) primary antibodies and IRDye 800CW conjugated secondary antibodies (Odyssey 926-32214; 1:10000). Signal was detected using a Li-Cor infra-red scanner (Odyssey).

Microscopy and image analysis. Cells for immunofluorescence were paraformaldehyde fixed, stained and fluorescence and transmitted light images of melanocytes were then collected using a Zeiss LSM710 confocal microscope fitted with a 63x 1.4NA oil immersion Apochromat lens. All images presented are single sections in the *z*-plane. Antibodies and stains were used as indicated; mouse monoclonal anti-GFP (Roche 11814460001; 1:300) rabbit-anti-tyrosinase (kindly supplied by Dr Vincent Hearing (NCI-NIH, USA) ; 1:100), rabbit-anti-giantin (Abcam 24586; 1:1000), mouse-anti-tubulin clone DM1a (Calbiochem cp06; 1:100), goat anti-mouse Alexa488 and goat anti-rabbit Alexa568 labelled secondary antibodies (Invitrogen A-11001 and A-11011; both 1:500). For live-cell visualisation of mitochondria melanocytes in μ-slide 8-well glass bottomed chamber slides (Ibidi IB-80827) were incubated for 30 minutes with medium containing 200nM MitoTracker® Red CMXRos (Invitrogen M7512). For analysis of melanosome clustering siRNA transfections were carried out in triplicate i.e. 3 wells of a 24-well plate for each siRNA in each experiment. 72 hours later phase contrast images of 3 different randomly-selected fields of cells in each well were captured using Axiovision 4.8 software associated with a Zeiss Axiovert 100S inverted microscope fitted with a 10x objective and an Axiocam CCD camera. Images were then randomised and the number of cells with clustered melanosomes in each field was counted by a researcher blinded to the identity of the siRNA transfected into each field of cells. Cells in which pigmented melanosomes were contained within the perinuclear cytoplasm (<50% of the total cytoplasmic area) were defined as containing clustered melanosomes. Measurement of the function of chimeric Kif5b fusion proteins in melanosome transport (Figure 5) was based on manual measurement of the proportion of cell area occupied by pigmented melanosomes as previously described (Hume et al., 2006).

Acknowledgements.

We thank Dr Stefan Linder (Univeristy of Hamburg, Germany) and Dr Chen Gu (Ohio State University, USA) for Kif5b vectors, Dr Sean Munro for SKIP vector, Dr Vincent Hearing (NCI-NIH, USA) for tyrosinase specific antibodies, Tim Self (confocal microscopy), Sue Cooper and Carol Sculthorpe (general) (all University of Nottingham, UK) for technical assistance and Andrew Foulkes and Jasmine Harris for carrying out corroborative studies.

Competing interests.

The authors declare no competing or financial interests.

Author contribution

CR, RDE, DAB and ANH conducted the experiments; ANH, CR and RDE designed the studies and wrote the paper.

Funding.

This work was supported by a Medical Research Council New Investigator Award to AH (grant reference G1100063) and a Biotechnology and Biological Sciences Research Council and University of Nottingham funded PhD studentship awarded to CR.

References.

AIZAWA, M. & FUKUDA, M. 2015. Small GTPase Rab2B and Its Specific Binding Protein Golgi-associated Rab2B Interactor-like 4 (GARI-L4) Regulate Golgi Morphology. *J Biol Chem,* 290**,** 22250-61.

ALBERTS, B., JOHNSON, A., LEWIS, J., RAFF, M., ROBERTS, K. & WALTER, P. 2008. *Molecular Biology of the Cell*, Garland Science.

BARLAN, K., ROSSOW, M. J. & GELFAND, V. I. 2013. The journey of the organelle: teamwork and regulation in intracellular transport. *Curr Opin Cell Biol,* 25**,** 483-8.

BYERS, H. R., YAAR, M., ELLER, M. S., JALBERT, N. L. & GILCHREST, B. A. 2000. Role of cytoplasmic dynein in melanosome transport in human melanocytes. *J Invest Dermatol,* 114**,** 990-7.

DUMONT, A., BOUCROT, E., DREVENSEK, S., DAIRE, V., GORVEL, J. P., POUS, C., HOLDEN, D. W. & MERESSE, S. 2010. SKIP, the host target of the Salmonella virulence factor SifA, promotes kinesin-1-dependent vacuolar membrane exchanges. *Traffic,* 11**,** 899-911.

EVANS, R. D., ROBINSON, C., BRIGGS, D. A., TOOTH, D. J., RAMALHO, J. S., CANTERO, M., MONTOLIU, L., PATEL, S., SVIDERSKAYA, E. V. & HUME, A. N. 2014. Myosin-Va and dynamic actin oppose microtubules to drive long-range organelle transport. *Curr Biol,* 24**,** 1743-50.

FUKUDA, M. 2013. Rab27 effectors, pleiotropic regulators in secretory pathways. *Traffic,* 14**,** 949-63.

FUKUDA, M., KURODA, T. S. & MIKOSHIBA, K. 2002. Slac2-a/melanophilin, the missing link between Rab27 and myosin Va: implications of a tripartite protein complex for melanosome transport. *J Biol Chem,* 277**,** 12432-6.

GOODE, B. L., DRUBIN, D. G. & BARNES, G. 2000. Functional cooperation between the microtubule and actin cytoskeletons. *Curr Opin Cell Biol,* 12**,** 63-71.

GROSS, S. P., TUMA, M. C., DEACON, S. W., SERPINSKAYA, A. S., REILEIN, A. R. & GELFAND, V. I. 2002. Interactions and regulation of molecular motors in Xenopus melanophores. *J Cell Biol,* 156**,** 855-65.

GU, C., ZHOU, W., PUTHENVEEDU, M. A., XU, M., JAN, Y. N. & JAN, L. Y. 2006. The microtubule plus-end tracking protein EB1 is required for Kv1 voltage-gated K+ channel axonal targeting. *Neuron,* 52**,** 803-16.

GUPTA, V., PALMER, K. J., SPENCE, P., HUDSON, A. & STEPHENS, D. J. 2008a. Kinesin-1 (uKHC/KIF5B) is required for bidirectional motility of ER exit sites and efficient ER-to-Golgi transport. *Traffic,* 9**,** 1850-66.

GUPTA, V., WERDENBERG, J. A., LAWRENCE, B. D., MENDEZ, J. S., STEPHENS, E. H. & GRANDE-ALLEN, K. J. 2008b. Reversible secretion of glycosaminoglycans and proteoglycans by cyclically stretched valvular cells in 3D culture. *Ann Biomed Eng,* 36**,** 1092-103.

HAMMER, J. A., 3RD & SELLERS, J. R. 2012. Walking to work: roles for class V myosins as cargo transporters. *Nat Rev Mol Cell Biol,* 13**,** 13-26.

HARA, M., YAAR, M., BYERS, H. R., GOUKASSIAN, D., FINE, R. E., GONSALVES, J. & GILCHREST, B. A. 2000. Kinesin participates in melanosomal movement along melanocyte dendrites. *J Invest Dermatol,* 114**,** 438-43.

HIROKAWA, N., NODA, Y., TANAKA, Y. & NIWA, S. 2009. Kinesin superfamily motor proteins and intracellular transport. *Nat Rev Mol Cell Biol,* 10**,** 682-96.

HOLUBCOVA, Z., HOWARD, G. & SCHUH, M. 2013. Vesicles modulate an actin network for asymmetric spindle positioning. *Nat Cell Biol,* 15**,** 937-47.

HUME, A. N., COLLINSON, L. M., RAPAK, A., GOMES, A. Q., HOPKINS, C. R. & SEABRA, M. C. 2001. Rab27a regulates the peripheral distribution of melanosomes in melanocytes. *J Cell Biol,* 152**,** 795-808.

HUME, A. N. & SEABRA, M. C. 2011. Melanosomes on the move: a model to understand organelle dynamics. *Biochem Soc Trans,* 39**,** 1191-6.

HUME, A. N., TARAFDER, A. K., RAMALHO, J. S., SVIDERSKAYA, E. V. & SEABRA, M. C. 2006. A coiled-coil domain of melanophilin is essential for Myosin Va recruitment and melanosome transport in melanocytes. *Mol Biol Cell,* 17**,** 4720-35.

HUME, A. N., USHAKOV, D. S., TARAFDER, A. K., FERENCZI, M. A. & SEABRA, M. C. 2007. Rab27a and MyoVa are the primary Mlph interactors regulating melanosome transport in melanocytes. *J Cell Sci,* 120**,** 3111-22.

HUME, A. N., WILSON, M. S., USHAKOV, D. S., FERENCZI, M. A. & SEABRA, M. C. 2011. Semi-automated analysis of organelle movement and membrane content: understanding rab-motor complex transport function. *Traffic,* 12**,** 1686-701.

ISHIDA, M., OHBAYASHI, N. & FUKUDA, M. 2015. Rab1A regulates anterograde melanosome transport by recruiting kinesin-1 to melanosomes through interaction with SKIP. *Sci Rep,* 5**,** 8238.

ISHIDA, M., OHBAYASHI, N., MARUTA, Y., EBATA, Y. & FUKUDA, M. 2012. Functional involvement of Rab1A in microtubule-dependent anterograde melanosome transport in melanocytes. *J Cell Sci,* 125**,** 5177-87.

KAPITEIN, L. C., VAN BERGEIJK, P., LIPKA, J., KEIJZER, N., WULF, P. S., KATRUKHA, E. A., AKHMANOVA, A. & HOOGENRAAD, C. C. 2013. Myosin-V opposes microtubule-based cargo transport and drives directional motility on cortical actin. *Curr Biol,* 23**,** 828-34.

KARDON, J. R. & VALE, R. D. 2009. Regulators of the cytoplasmic dynein motor. *Nat Rev Mol Cell Biol,* 10**,** 854-65.

LINSTEDT, A. D. & HAURI, H. P. 1993. Giantin, a novel conserved Golgi membrane protein containing a cytoplasmic domain of at least 350 kDa. *Mol Biol Cell,* 4**,** 679-93.

LO PRESTI, L. & MARTIN, S. G. 2011. Shaping fission yeast cells by rerouting actin-based transport on microtubules. *Curr Biol,* 21**,** 2064-9.

MARCHESIN, V., CASTRO-CASTRO, A., LODILLINSKY, C., CASTAGNINO, A., CYRTA, J., BONSANG-KITZIS, H., FUHRMANN, L., IRONDELLE, M., INFANTE, E., MONTAGNAC, G., REYAL, F., VINCENT-SALOMON, A. & CHAVRIER, P. 2015. ARF6-JIP3/4 regulate endosomal tubules for MT1-MMP exocytosis in cancer invasion. *J Cell Biol,* 211**,** 339-58.

MATSUI, T., OHBAYASHI, N. & FUKUDA, M. 2012. The Rab interacting lysosomal protein (RILP) homology domain functions as a novel effector domain for small GTPase Rab36: Rab36 regulates retrograde melanosome transport in melanocytes. *J Biol Chem,* 287**,** 28619-31.

NAVONE, F., NICLAS, J., HOM-BOOHER, N., SPARKS, L., BERNSTEIN, H. D., MCCAFFREY, G. & VALE, R. D. 1992. Cloning and expression of a human kinesin heavy chain gene: interaction of the COOH-terminal domain with cytoplasmic microtubules in transfected CV-1 cells. *J Cell Biol,* 117**,** 1263-75.

NUOFFER, C., DAVIDSON, H. W., MATTESON, J., MEINKOTH, J. & BALCH, W. E. 1994. A GDP-bound of rab1 inhibits protein export from the endoplasmic reticulum and transport between Golgi compartments. *J Cell Biol,* 125**,** 225-37.

OHBAYASHI, N., MARUTA, Y., ISHIDA, M. & FUKUDA, M. 2012. Melanoregulin regulates retrograde melanosome transport through interaction with the RILP-p150Glued complex in melanocytes. *J Cell Sci,* 125**,** 1508-18.

PROVANCE, D. W., JR., WEI, M., IPE, V. & MERCER, J. A. 1996. Cultured melanocytes from dilute mutant mice exhibit dendritic morphology and altered melanosome distribution. *Proc Natl Acad Sci U S A,* 93**,** 14554-8.

PRUYNE, D., LEGESSE-MILLER, A., GAO, L., DONG, Y. & BRETSCHER, A. 2004. Mechanisms of polarized growth and organelle segregation in yeast. *Annu Rev Cell Dev Biol,* 20**,** 559-91.

RAPOSO, G. & MARKS, M. S. 2007. Melanosomes--dark organelles enlighten endosomal membrane transport. *Nat Rev Mol Cell Biol,* 8**,** 786-97.

ROGERS, S. L. & GELFAND, V. I. 1998. Myosin cooperates with microtubule motors during organelle transport in melanophores. *Curr Biol,* 8**,** 161-4.

ROSA-FERREIRA, C. & MUNRO, S. 2011. Arl8 and SKIP act together to link lysosomes to kinesin-1. *Dev Cell,* 21**,** 1171-8.

ROSS, J. L., ALI, M. Y. & WARSHAW, D. M. 2008. Cargo transport: molecular motors navigate a complex cytoskeleton. *Curr Opin Cell Biol,* 20**,** 41-7.

SCHLIWA, M. & EUTENEUER, U. 1978. A microtuble-independent component may be involved in granule transport in pigment cells. *Nature,* 273**,** 556-8.

SCHUH, M. 2011. An actin-dependent mechanism for long-range vesicle transport. *Nat Cell Biol,* 13**,** 1431-6.

SEGEV, N., MULHOLLAND, J. & BOTSTEIN, D. 1988. The yeast GTP-binding YPT1 protein and a mammalian counterpart are associated with the secretion machinery. *Cell,* 52**,** 915-24.

TANAKA, Y., KANAI, Y., OKADA, Y., NONAKA, S., TAKEDA, S., HARADA, A. & HIROKAWA, N. 1998. Targeted disruption of mouse conventional kinesin heavy chain, kif5B, results in abnormal perinuclear clustering of mitochondria. *Cell,* 93**,** 1147-58.

TISDALE, E. J., BOURNE, J. R., KHOSRAVI-FAR, R., DER, C. J. & BALCH, W. E. 1992. GTP-binding mutants of rab1 and rab2 are potent inhibitors of vesicular transport from the endoplasmic reticulum to the Golgi complex. *J Cell Biol,* 119**,** 749-61.

VANCOILLIE, G., LAMBERT, J., MULDER, A., KOERTEN, H. K., MOMMAAS, A. M., VAN OOSTVELDT, P. & NAEYAERT, J. M. 2000a. Cytoplasmic dynein colocalizes with melanosomes in normal human melanocytes. *Br J Dermatol,* 143**,** 298-306.

VANCOILLIE, G., LAMBERT, J., MULDER, A., KOERTEN, H. K., MOMMAAS, A. M., VAN OOSTVELDT, P. & NAEYAERT, J. M. 2000b. Kinesin and kinectin can associate with the melanosomal surface and form a link with microtubules in normal human melanocytes. *J Invest Dermatol,* 114**,** 421-9.

WEI, Q., WU, X. & HAMMER, J. A., 3RD 1997. The predominant defect in dilute melanocytes is in melanosome distribution and not cell shape, supporting a role for myosin V in melanosome transport. *J Muscle Res Cell Motil,* 18**,** 517-27.

WILSON, B. S., NUOFFER, C., MEINKOTH, J. L., MCCAFFERY, M., FERAMISCO, J. R., BALCH, W. E. & FARQUHAR, M. G. 1994. A Rab1 mutant affecting guanine nucleotide exchange promotes disassembly of the Golgi apparatus. *J Cell Biol,* 125**,** 557-71.

WOOLNER, S. & BEMENT, W. M. 2009. Unconventional myosins acting unconventionally. *Trends Cell Biol,* 19**,** 245-52.

WU, X., BOWERS, B., RAO, K., WEI, Q. & HAMMER, J. A., 3RD 1998. Visualization of melanosome dynamics within wild-type and dilute melanocytes suggests a paradigm for myosin V function In vivo. *J Cell Biol,* 143**,** 1899-918.

WU, X. S., RAO, K., ZHANG, H., WANG, F., SELLERS, J. R., MATESIC, L. E., COPELAND, N. G., JENKINS, N. A. & HAMMER, J. A., 3RD 2002. Identification of an organelle receptor for myosin-Va. *Nat Cell Biol,* 4**,** 271-8.

WU, X. S., TSAN, G. L. & HAMMER, J. A., 3RD 2005. Melanophilin and myosin Va track the microtubule plus end on EB1. *J Cell Biol,* 171**,** 201-7.

Figures

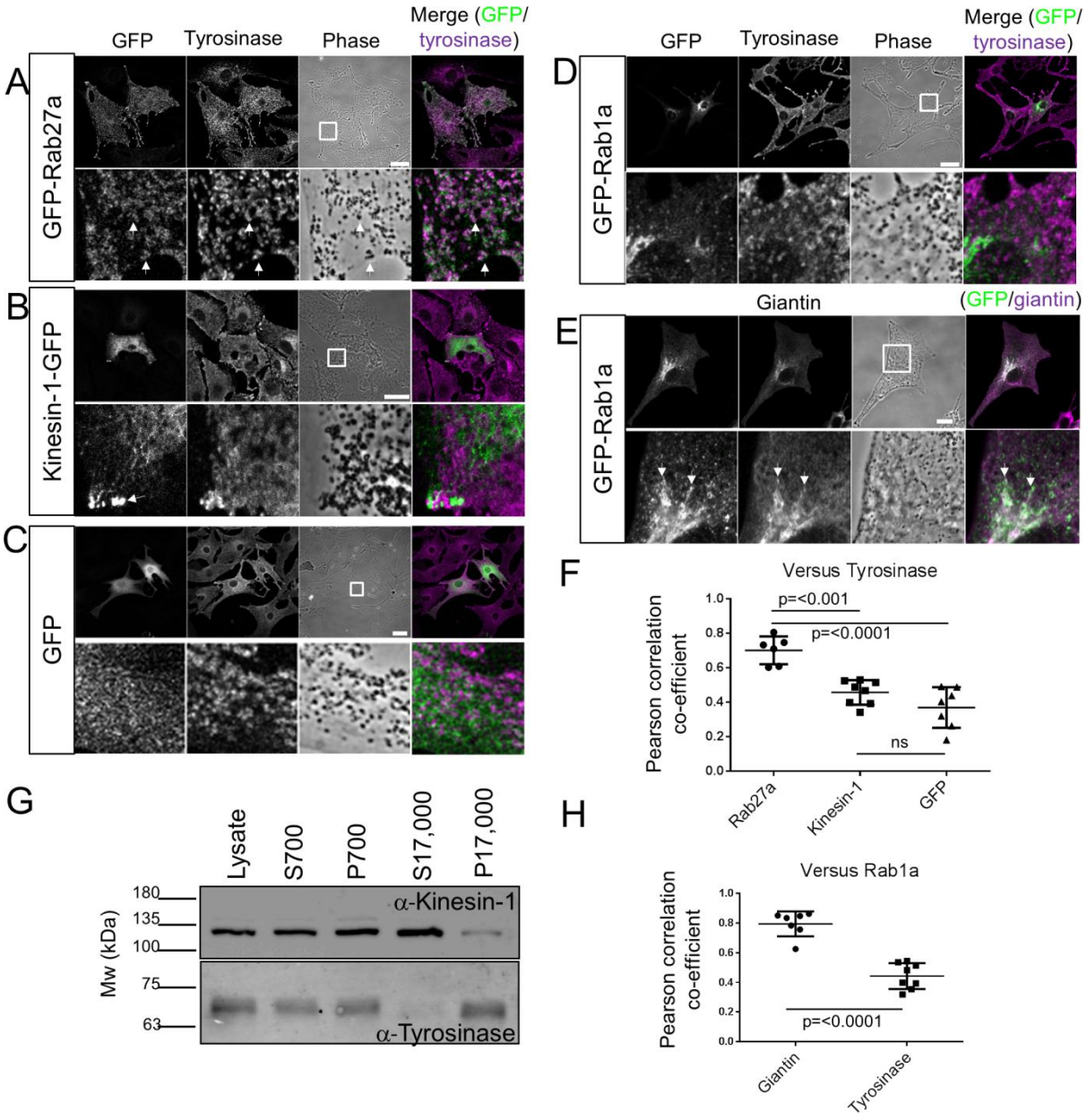

Figure 1. The intracellular distribution of Kif5b and Rab1a in mouse melanocytes. melan-a cells were transiently transfected with plasmid vectors allowing the expression of the indicated GFP fusion proteins. Cells were fixed after 48 hours, stained with the indicated organelle marker specific antibodies and the intracellular distribution of GFP and organelle markers was observed using a confocal microscope (as described in material and methods). (A-E) are single confocal z-sections

showing the distribution of GFP-Rab27a (A), Kif5b-GFP (B), GFP (C) and GFP-Rab1a (D-E) relative to organelle markers. Tyrosinase marks melanosomes (A-D) and giantin marks the Golgi apparatus (E), respectively. Phase/transmitted light images show the distribution of pigmented melanosomes. In merge images GFP is coloured green, organelle markers are coloured magenta thus white pixels indicate colocalisation. The white squares in the phase images indicate the part of the cell that is presented in the high magnification panels below. Arrows in A and E highlight areas of colocalisation while the arrows in B indicate the accumulation of Kif5b-YFP at the peripheral +tips of microtubules. Scale bar = 20μm. (F and H) are scatter plots showing the extent of co-localisation (measured using the Pearson correlation co-efficient (PCC)) between tyrosinase and Rab27a (n=6), Kif5b (n=8) and GFP (n=7) (F), and between GFP-Rab1a and tyrosinase (n=8) or giantin (n=7) in melan-a cells (H). Significance testing was using one-way ANOVA and the significance of differences in PCC values between populations is indicated. (G) Western blots showing the expression of Kif5b and tyrosinase in sub-cellular fractions of melan-a cells (as described in material and methods).

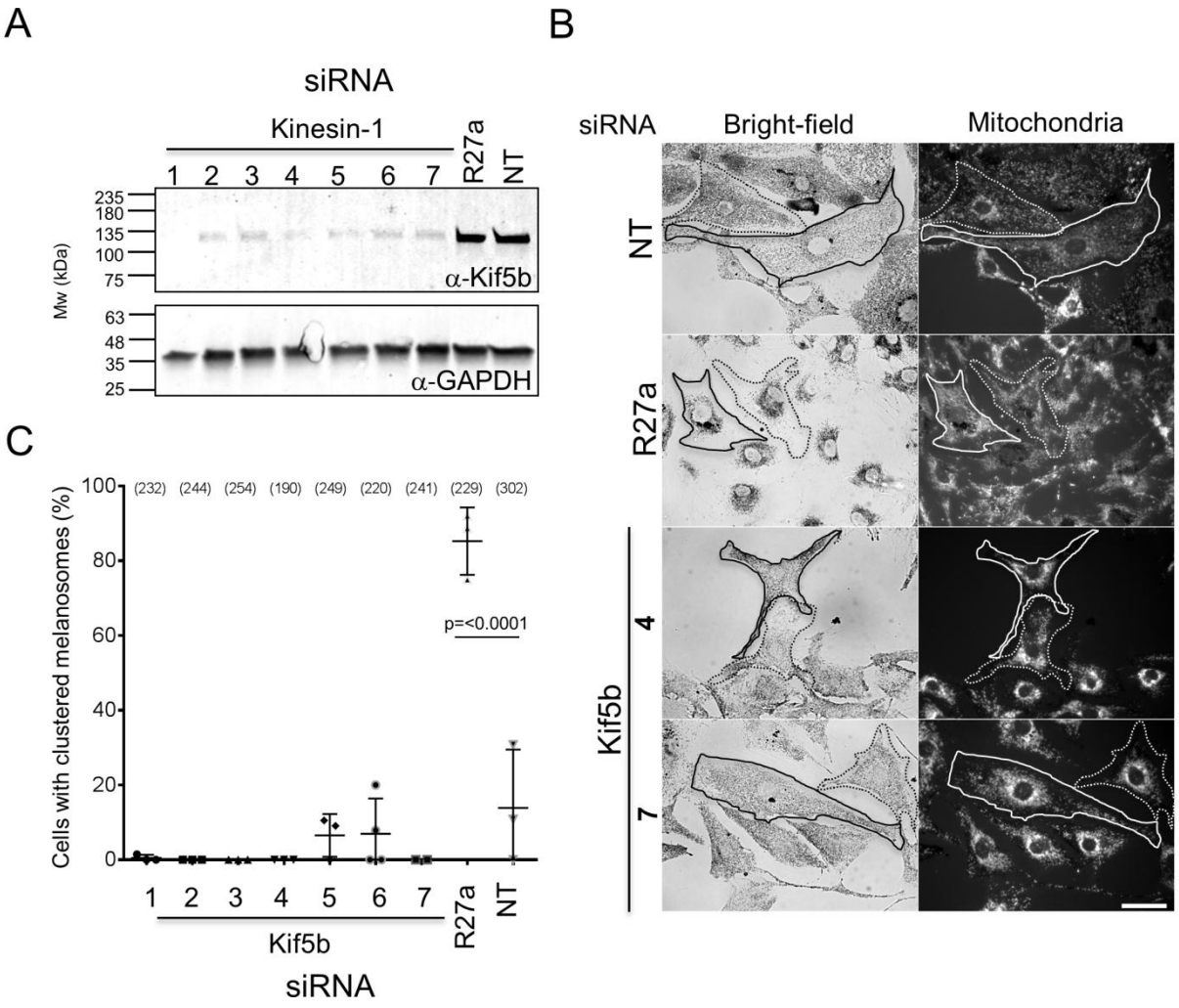

Figure 2. Knockdown of Kif5b in melanocytes affects distribution of mitochondria but not melanosomes. melan-a cells were transfected with the indicated siRNA and protein levels and melanosome clustering were measured (as described in material and methods). (A) Western blots showing the level of Kif5b and GAPDH (loading control) proteins in lysates of siRNA transfected cells. The blot displayed is representative of 3 independent blots from 3 independent transfections. (B) Representative bright-field and fluorescence images (left and right panels) showing the sub-cellular distribution of melanosomes and mitochondria, respectively, in fields of siRNA transfected melanocytes. Traces indicate cell borders to highlight clustering of mitochondria in Kif5b versus Rab27a and control siRNA transfected cells. Scale bar = 20μm. (C) A scatter plot showing the percentage of melanocytes manifesting perinuclear clustered melanosomes for each siRNA. Data are

from 3 independent transfections each performed in triplicate on different pools of cells. Plotted points represent the average percentage of cells with perinuclear clustered melanosomes from each experiment (as described in material and methods). Bracketed numbers indicate the total number of cells analysed.

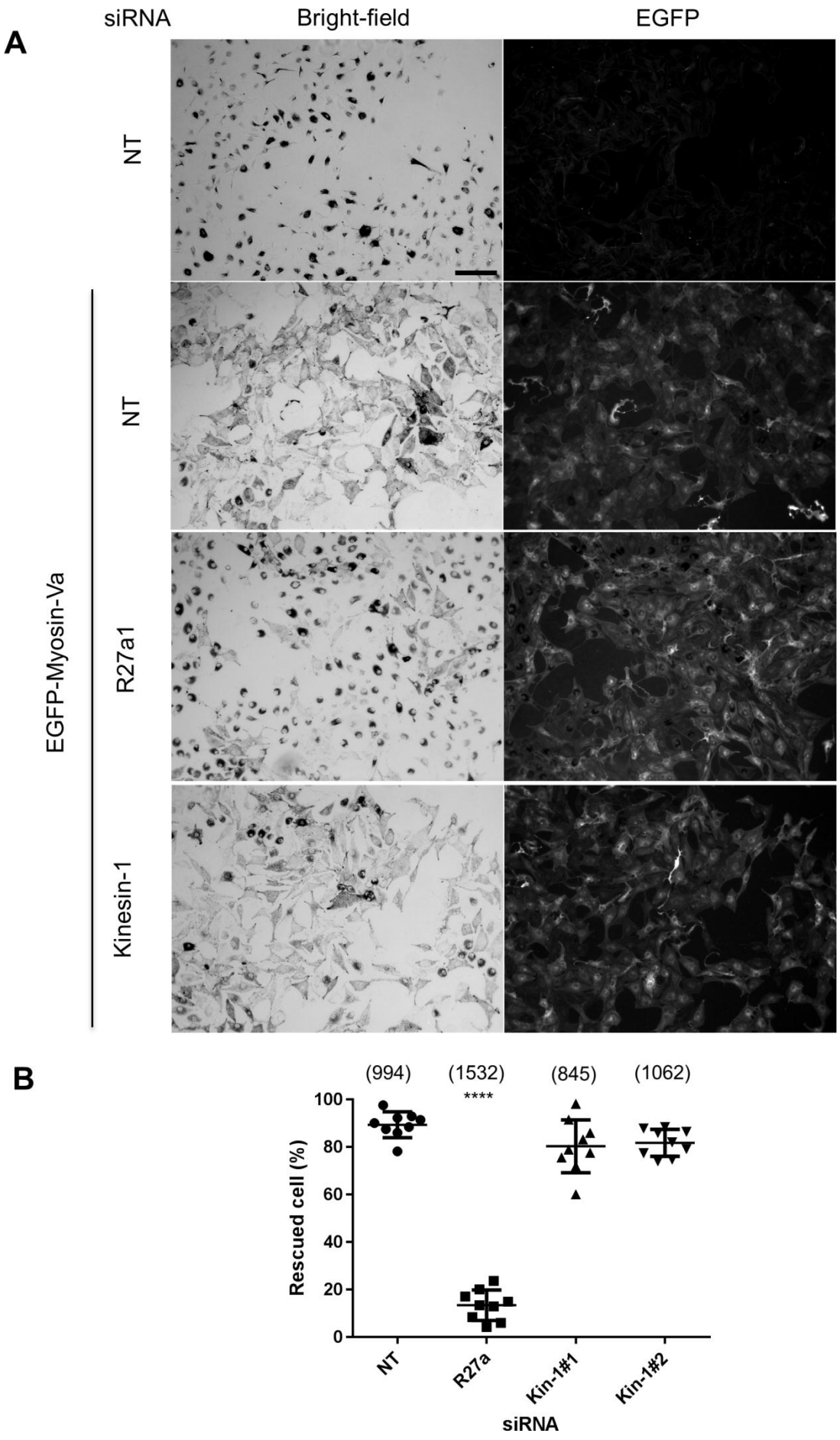

Figure 3. Knockdown of Kif5b does not compromise myosin-Va driven centrifugal melanosome transport. melan-d1 cells were transfected with the indicated siRNA, then 72 hours later infected with GFP-myosin-Va expressing adenovirus, fixed and stained with anti-GFP antibodies to reveal the expression of myosin-Va (as described in material and methods). (A) Representative low-power bright-field and corresponding fluorescence images showing the sub-cellular distribution of melanosomes and expression of GFP-myosin-Va in fields of siRNA transfected/GFP-myosin-Va expressing melan-d1 cells. Scale bar = 100μm. (B) A scatter plot showing the percentage of melanocytes manifesting perinuclear clustered melanosomes for each siRNA. Data are from 9 independent transfections each performed in triplicate on different pools of cells. Plotted points represent the average percentage of cells with perinuclear clustered melanosomes from each experiment (as described in material and methods). Bracketed numbers indicate the total number of cells analysed. **** indicates p=<0.0001 relative to NT transfected cells determine by one-way ANOVA, no other significant differences were observed.

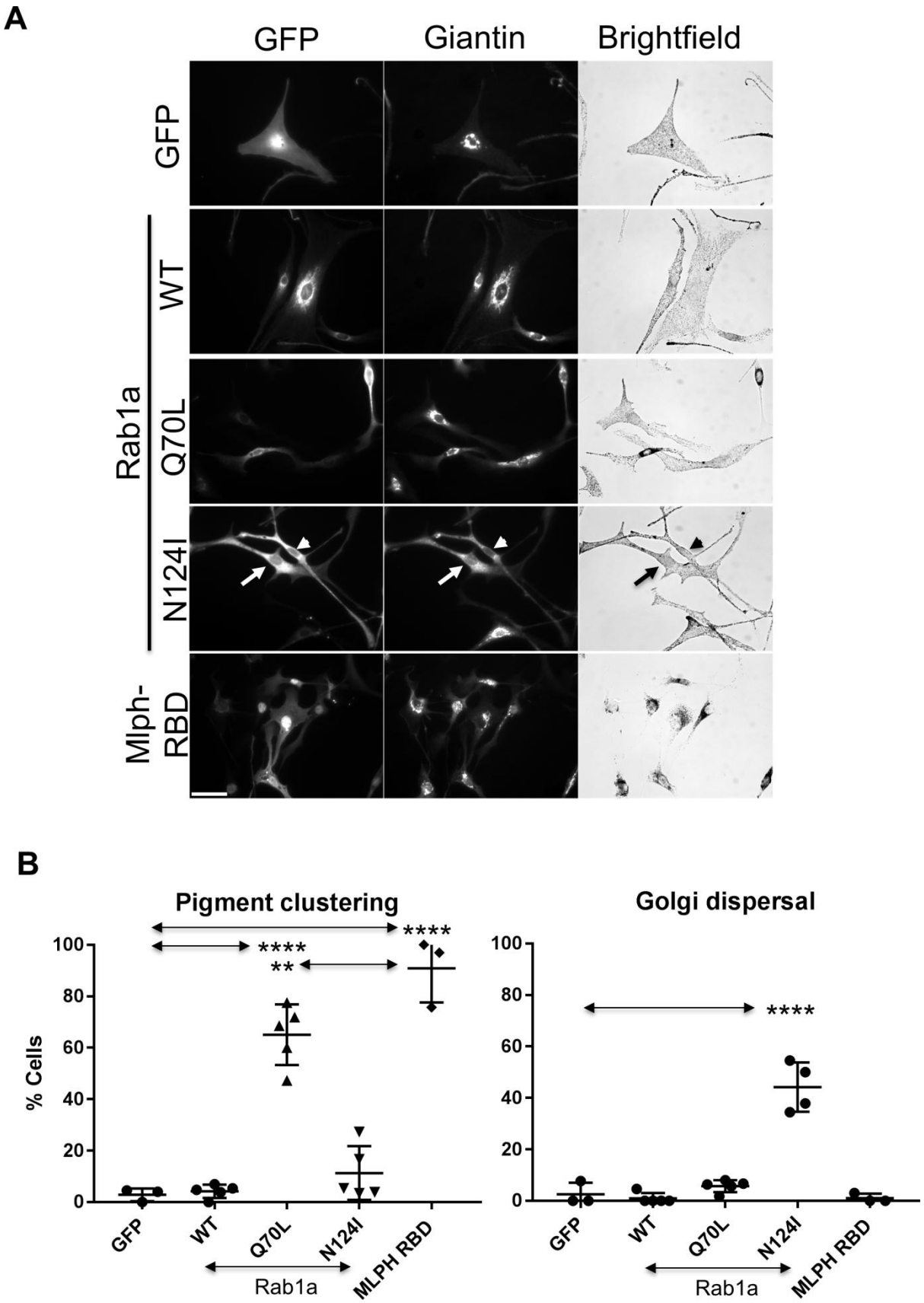

Figure 4. Expression of a dominant negative Rab1a^{N124I} mutant affects Golgi integrity but not melanosome distribution. melan-a cells were infected with adenovirus vectors allowing expression of the indicated proteins, fixed and stained with giantin specific antibodies to reveal the structure of the Golgi apparatus (as described in material and methods). (A) Representative fluorescence and bright-field micrographs showing the distribution of GFP-tagged protein, giantin/Golgi and melanosome in infected melanocytes. For the Rab1a^{N124I} mutant the arrow and arrowhead indicate the cells expressing mutant protein. Scale bar = 40μm. (B) A scatter plot showing the percentage of melanocytes expressing each protein in which melanosomes were clustered in the perinuclear cytoplasm. Data are from 3 (GFP and Mlph-RBD) or 5 (Rab1a and mutants) independent experiments. Plotted points represent the average percentage of cells with perinuclear clustered melanosomes from each experiment (as described in material and methods). Total number of cells analysed; GFP = 73, Rab1a^{WT} = 153, Rab1a^{Q70L} = 196, Rab1a^{N124I} = 132 and Mlph-RBD = 167. **** and ** indicate p=<0.0001 and p=<0.01, respectively as determined by one-way ANOVA, arrows indicate compared datasets. No other significant differences were observed.

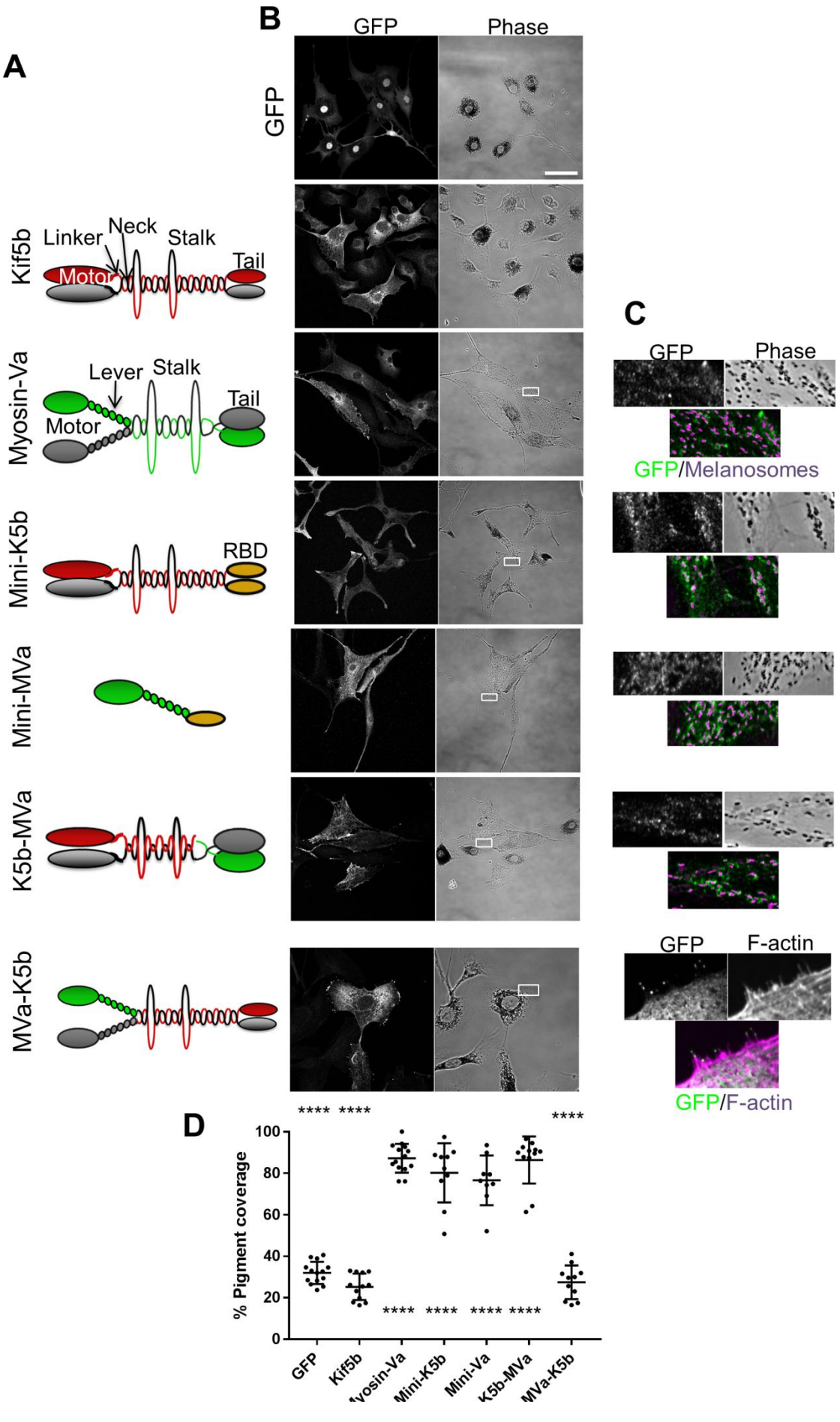

Figure 5. Forced targeting of Kif5b to melanosomes can drive centrifugal melanosome transport in melanocytes. melan-d1 cells were infected with adenovirus allowing expression of the indicated GFP fusion proteins then 24 hours later fixed, processed for immunofluorescence and imaged using a confocal microscope (as described in material and methods). A) (left-hand column) are schematics representations of the domain organisation and expected oligomeric state of the Kif5b (red and grey shapes), myosin-Va (green and grey shapes) and fusion proteins. RBD (orange shape) indicates Rab27a binding domain of murine Sytl2-a (as described in previously (Evans et al., 2014)). B) (middle column) Pairs of confocal fluorescence and phase contrast (transmitted light) images showing the distribution of GFP fusion proteins and melanosomes, respectively) in representative fields of infected cells. Scale bar = 50μm. C) (right-hand column) high magnification images of cells within the borders of the white boxes in lower magnification images (B) phase images indicate the areas shown that highlight association between fusion proteins (green) and F-actin (MVa-K5b) and melanosomes, both magenta (others). B) A scatter plot showing the pigment distribution in as reported by % pigment coverage (pigment filled area/total cell area) was calculated as described previously [Hume 2006]. Horizontal bars show the median and 25th and 75th percentile of the each population. The significance of differences in pigment coverage for each population compared with the GFP and wildtype myosin-Va are displayed below and above each scatter (**** indicates p=<0.0001), respectively as determined by one-way ANOVA. No other significant differences were observed. Data are from one of three independent experiments and are representative of the results the all experiments. Number of cells analysed; GFP = 14, Kif5b = 12, myosin-Va = 14, mini-K5b = 10, mini-Va = 9, k5b-mva = 12 and mVa-k5b = 11.

siRNA	Sense pirmer sequence 5'-3'	Reference.
Kif5b - 1	TGACCAGAATTCTTCAAGA	(Ishida et al., 2015)
Kif5b - 2	GCAGTCAGGTCAAAGAACA	(Ishida et al., 2015)
Kif5b - 3	AGAAGGAACUGGUAUGAUA	This study.
Kif5b - 4	CAACAGACAUGUCGCAGUU	This study.
Kif5b - 5	GGAGGAGGCUCAUUUGUUC	This study.
Kif5b - 6	GAAACGAGCAGCUGAAAUG	This study.
Kif5b - 7	UGAAUUGCUUAGUGAUGAA	(Gupta et al., 2008b)
Rab27a	GGAGAGGUUUCGUAGCUUA	(Hume et al., 2007)
NT	UAAGGCUAUGAAGAGAUAC	Dharmacon D-001210-02

Table 1. siRNA used in this study.

Supplementary Information

Supplementary figure 1

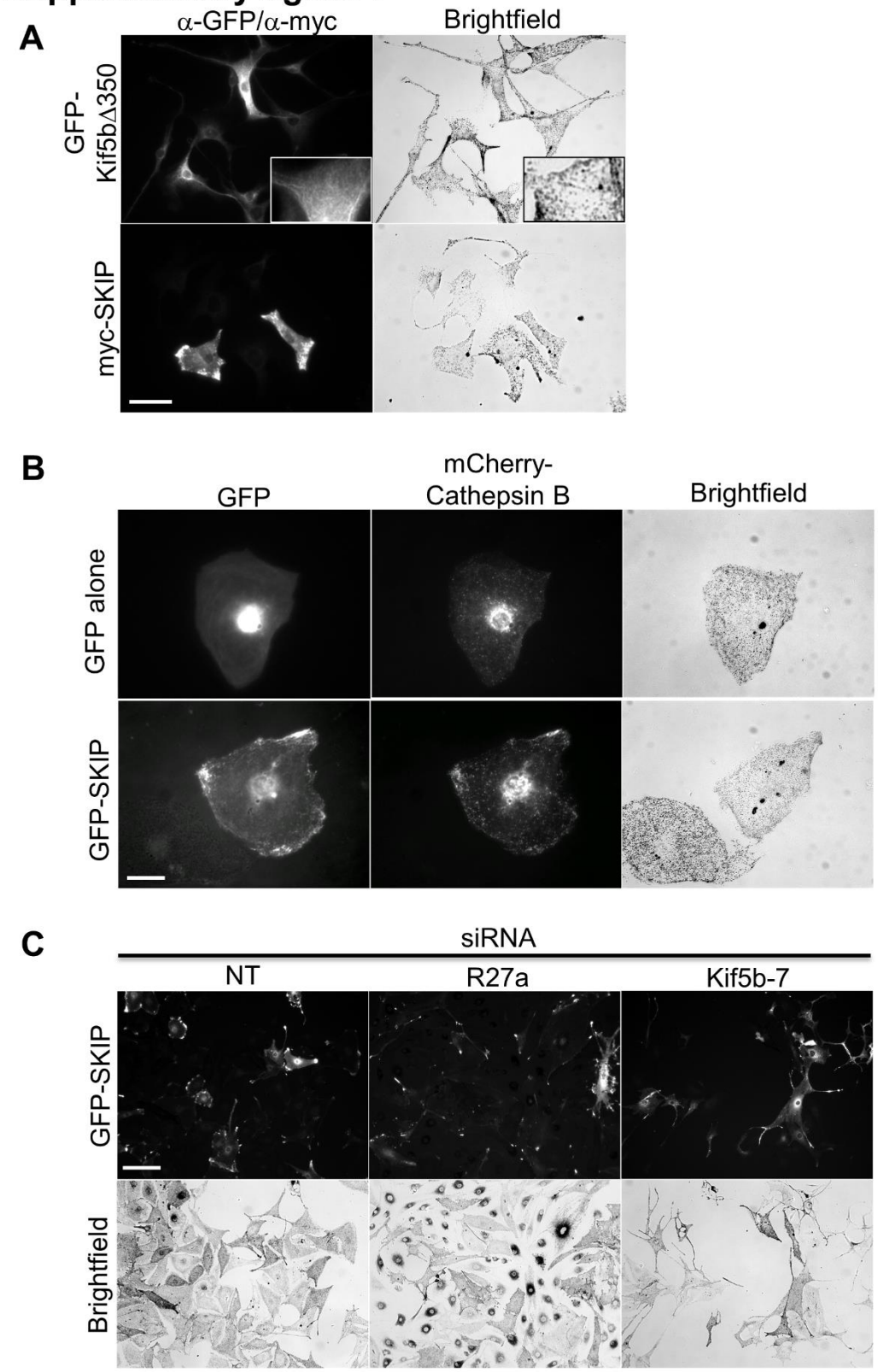

Figure S1. Expression of motor-less Kif5b (GFP-Kif5bΔ350) and myc/GFP-tagged SKIP in melanocytes. melan-a cells were transiently transfected with plasmid vectors allowing expression of the indicated fusion proteins, fixed 48 hours later, processed for immunofluroscence and imaged using a fluorescence microscope (as described in materials and methods). Fluorscence and bright-field images show the distribution of heterologously expressed/endogenous protein and melanosomes in transfected cells. A) Neither motor-less Kif5b (GFP-Kif5bΔ350) nor myc-tagged SKIP co-localise with melanosomes. B) Expression of SKIP in melanocytes disperses lysosomes but not melanosomes. C) melan-a cells transfected with siRNA (as indicated) were infected with adenovirus vectors allowing expression of GFP-SKIP 72h after transfection and fixed and processed for immunofluorescence 24h later (as described in materials and methods). Scale bar (A) = 50μm, (B) = 20μm and (C) =100μm.

Supplementary Figure 2

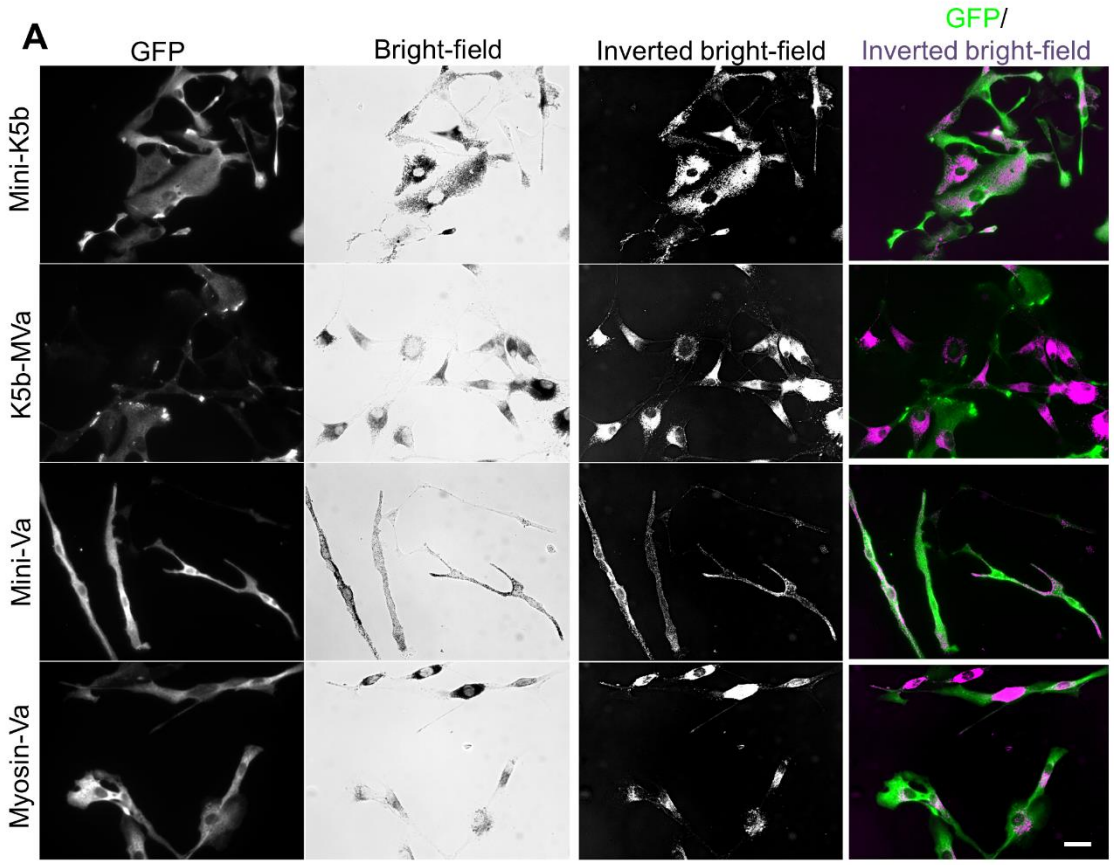

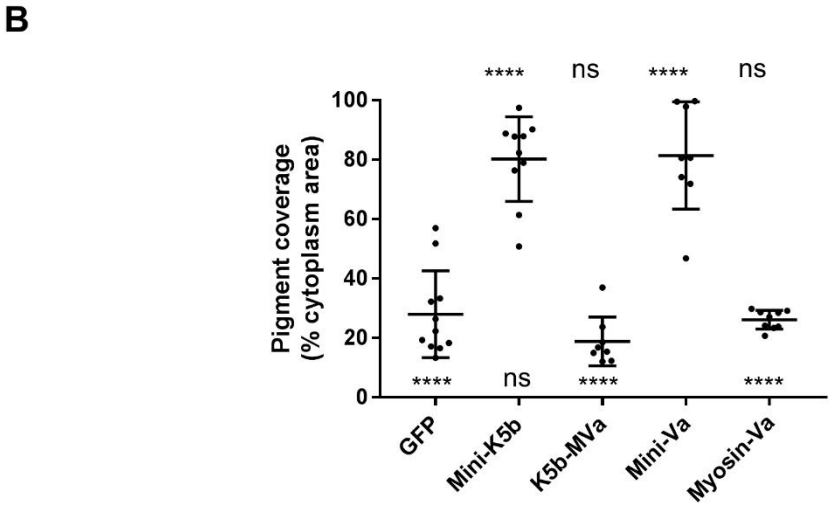

Figure S2. The function of the K5b-MVa, but not the mini-K5b, fusion protein is dependent upon melanophilin expression. Melanophilin null (melan-ln) cells were infected with adenovirus vectors allowing expression of the indicated GFP fusion proteins, fixed 24 hours later, processed for immunofluorescence and imaged using a confocal microscope (as described in material and methods). A) Fluorescence (green in merge), bight-field, inverted bright-field (magenta in merge) and merged images showing the distribution of the GFP fused motor proteins and melanosomes in representative fields of infected melan-ln cells. Scale bar = 20□m. B) A scatter plot showing the pigment distribution as reported by pigment coverage (% pigment filled area/total cell area) was calculated as described previously (Hume et al 2006). Horizontal bars show the median and 25th and 75th percentile of each population. The significance of differences in pigment coverage for each population compared with the GFP and mini-Va are displayed above and below each scatter (**** indicates p=<0.0001), respectively, as determined by one-way ANOVA. No other significant differences were observed. Data are from one of three independent experiments and are representative of the results of all experiments. Number of cells analysed; GFP = 11, myosin-Va = 9, mini-K5b = 10, mini-Va = 8 and K5b-MVa = 8.

Supplementary Figure 3

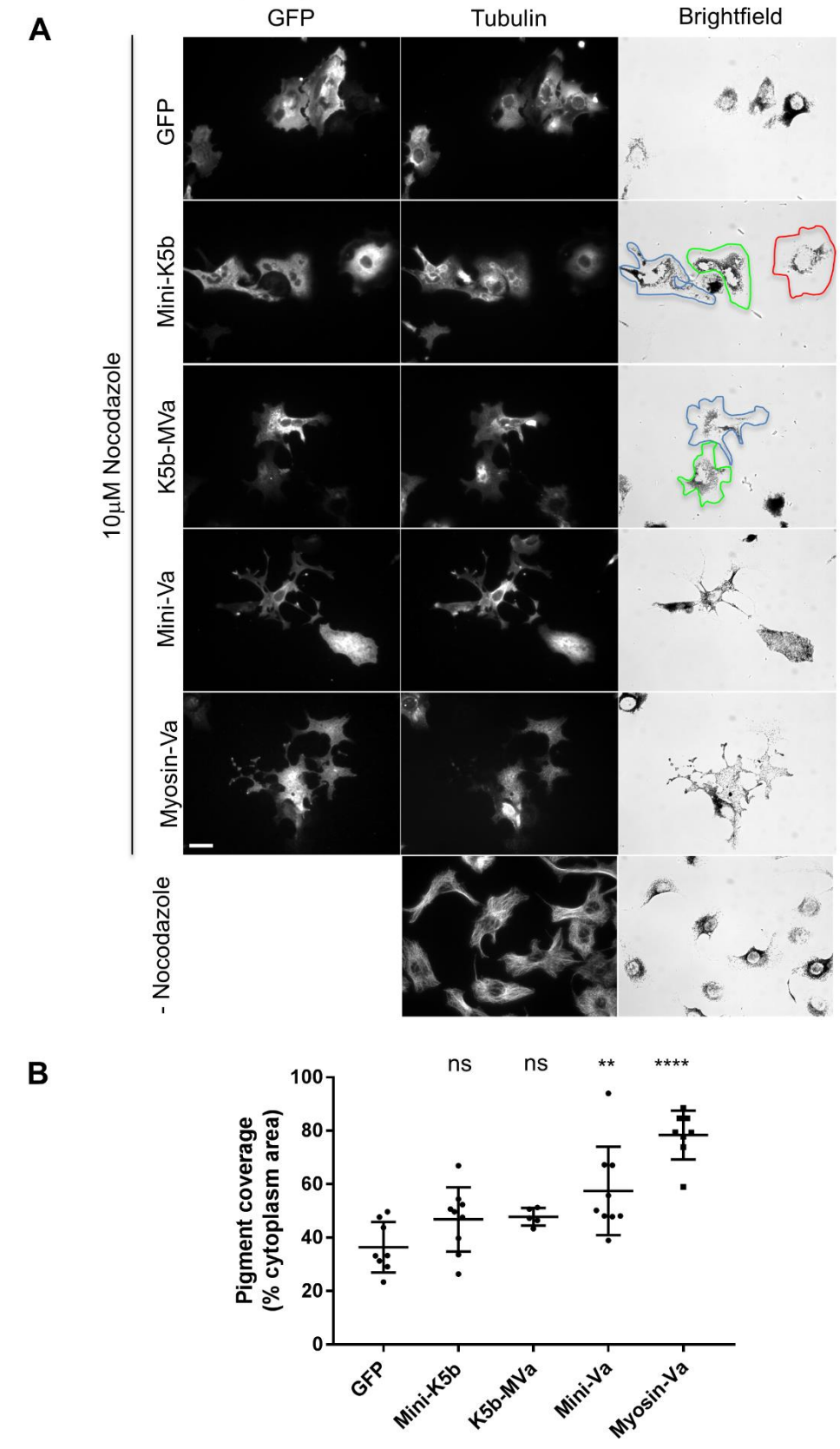

Figure S3. Kif5b containing motors are dependent upon microtubule integrity for function. melan-d1 cells were infected with adenoviruses allowing expression of the indicated GFP fusion proteins then 24 hours later fixed, processed for immunofluorescence and imaged using a confocal microscope (as described in material and methods). For 1 hour prior to, and throughout adenovirus incubation, cells were maintained in medium supplemented with 10μM nocozadole to deplete microtubules. A) Fluorescence and bright field images showing the intracellular distribution of GFP fusions, tubulin and melanosomes. For mini-K5b and K5b-MVa cell outline traces have been overlaid onto bright-field images to highlight clustered melanosome distribution. Scale bar = 20μm. B) A scatter plot showing the pigment distribution in as reported by pigment coverage (% pigment filled area/total cell area) was calculated as described previously [Hume 2006]. Horizontal bars show the median and 25th and 75th percentile of the each population. The significance of differences in pigment coverage for each population compared with the GFP are displayed above each scatter (**** indicates p=<0.0001), respectively, as determined by one-way ANOVA. Data are from one of three independent experiments and are representative of the results of all experiments. Number of cells analysed; GFP = 8, myosin-Va = 8, mini-K5b = 9, mini-Va = 9 and K5b-MVa = 5.

Supplementary Figure 4

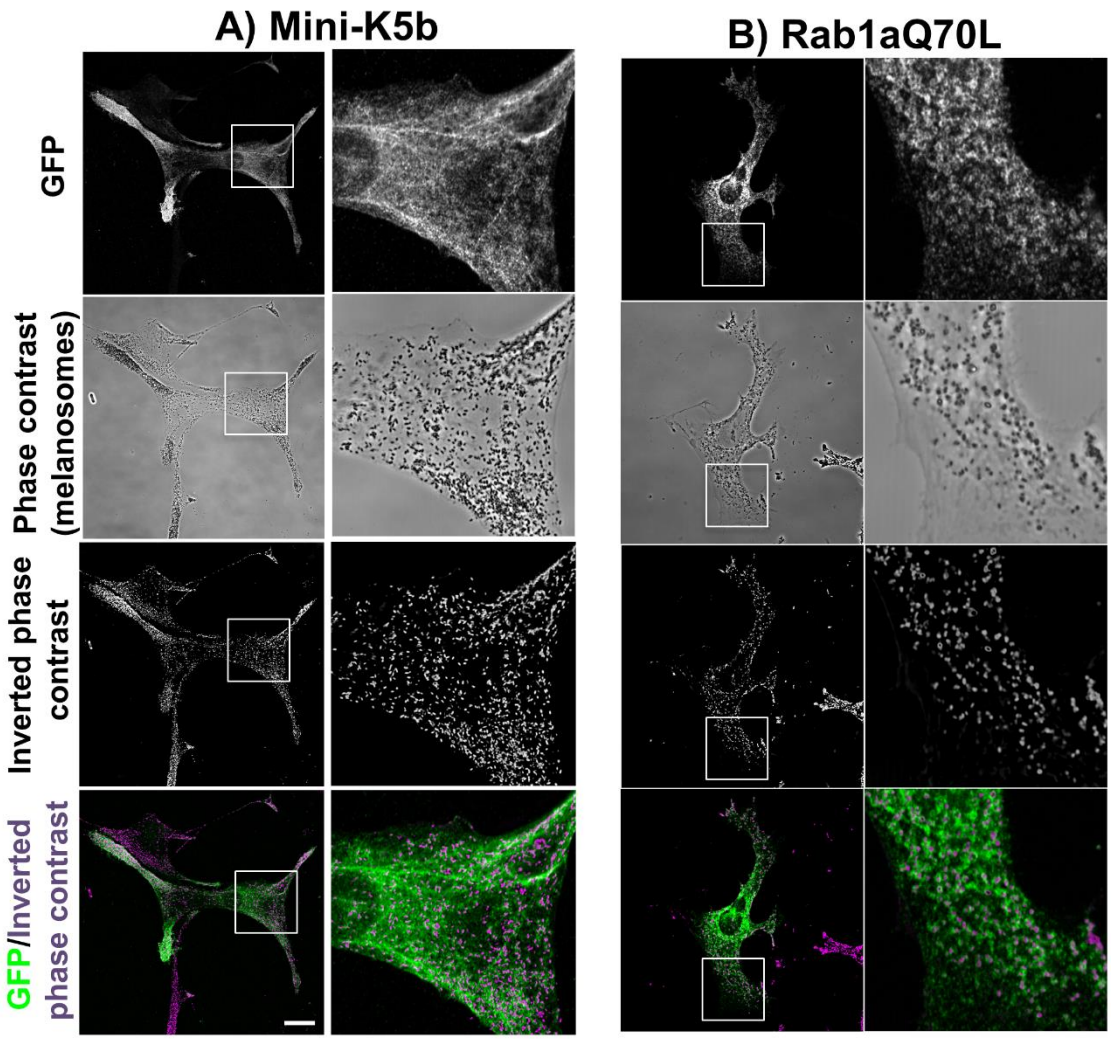

Figure S4. Expression of melanosome targeted mini-K5b (A) and constitutively active Rab1a^{Q70L} (B) in melanocytes. A) mini-K5b drives hyper-dispersion of melanosomes to the tips of dendrites in melanocytes. melan-a cells were infected with adenovirus allowing expression of the mini-K5b or GFP-Rab1a^{Q70L} melanosome targeted active Kif5b, fixed 24h later, prepared for immunofluorescence and imaged using a confocal microscope as described in material and methods. B) Constitutively active Rab1a^{Q70L} is localised to melanosomes in melanocytes. melan-a cells were transfected with plasmid vectors allowing expression, fixed 48 hours later, prepared for immunofluorescence and the distribution of fluorescence recorded using a confocal microscope, as described in materials and methods. White boxes in left-hand images indicate the region shown in high magnification images on the right-hand images. Scale bar = 20μm.